Self-Commissioning Algorithm for Inverter Non-Linearity Compensation in Sensorless Induction Motor Drives

Self-Commissioning Algorithm for Inverter Non-Linearity Compensation in Sensorless Induction Motor Drives

G. Pellegrino, P. Guglielmi, E. Armando and R. Bojoi
Politecnico di Torino, C.so Duca degli Abruzzi, 24
10129, Torino - Italy
Emails: (gianmario.pellegrino, paolo.guglielmi, eric.armando, radu.bojoi)@polito.it

ABSTRACT

In many Sensorless Field Oriented Control schemes for Induction Motor (IM) drives the flux is estimated by means of the measured motor currents and the control reference voltages. In most of cases, the flux estimation is based on the integral of the back-EMF voltages. The inverter nonlinear errors (dead-time and on-state voltage drops) introduce a distortion in the estimated voltage that reduces the accuracy of the flux estimation, particularly at low speed. In the literature, most of the compensation techniques of such errors require the off-line identification of the inverter model and off-line post-processing. The paper presents a simple and accurate method for the identification of the inverter parameters at the drive start-up. The method is integrated into the control code of the IM drive and it is based on the informations contained in the feedback signal of the flux observer. The procedure applies, more in general, to all those sensorless AC drives where the flux is estimated using the back-EMF integration, not only for IM drives but also permanent magnet synchronous motor drives (SMPM, IPM). The self-commissioning algorithm is presented and tested for the sensorless control of an induction motor drive, implemented on a fixed-point DSP. The feasibility and effectiveness of the method are demonstrated by experimental results.

I. INTRODUCTION

Sensorless Field Oriented Controlled (SFOC) IM drives are an expanding technology. The absence of the shaft sensor gives advantages in terms of cost and reliability. SFOC is applied not only to drives with good dynamics requirements (like spindle-drives or traction-drives) but it is also becoming popular in those fields where scalar V/Hz control was traditionally adopted (like pumps, fans and washing machines).

The key issue of the SFOC is to obtain an accurate estimation of the machine flux vector (either rotor or stator flux) in order to get a decoupled control of the machine excitation flux and torque.

The solutions proposed in the literature to estimate the flux by means of electrical quantities only (voltage and current vectors $\overline{v}_s$, $\overline{i}_s$) are based on the stator model of the motor, that is the time integral of the back-EMF voltages. Since open-loop integration is practically unstable, a negative feedback is needed to avoid the flux signal to drift due to input offset: in Fig.1 the block scheme of a generic flux observer is reported with the feedback signal $\overline{v}_\epsilon$ put in evidence. The observers/estimators of this kind are various: from simple low pass-filter estimators [1], [2] to closed loop observers [3], [4], [5].

The motor back-EMF estimation is obtained by means of the command vector ($\overline{v}_s^*$) minus the voltage drop on the estimated stator resistance ($\tilde{R}_s$). The use of the command voltages instead of the measured ones is a straightforward approach that improves the reliability and reduces the cost of the system. However, it introduces an error due to the inverter non-linear drops, that must be properly compensated, in particular at low speed.

At the drive start-up, in DC steady-state conditions, the flux observer feedback signal $\overline{v}_\epsilon$ contains useful informations about the inverter error, as will be demonstrated throughout the paper. The inverter voltage drops consist of a main non-linear term (dead-time, on-state threshold of the power switches), and a minor linear term (on-state resistance) that will be separately identified. The motor resistance (stator resistance) is also estimated during the identification procedure, as a whole with the on-state resistance of the inverter.

A well recognized model of the inverter non-idealities has been proposed in [6]. Effective techniques for feed-forward compensation based on that model are proposed in [6], [7] and [8]. A different scheme, by the same inverter model

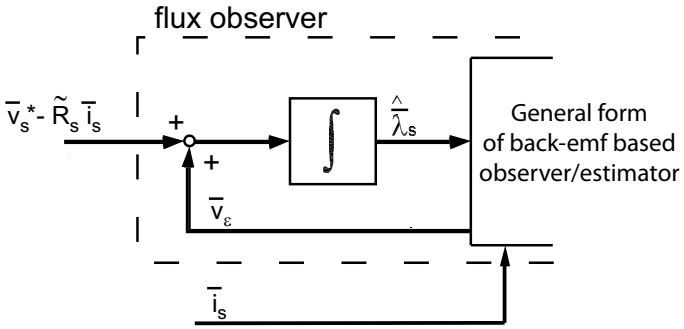

Fig. 1. General form of a closed-loop flux estimator based on the back-EMF voltage time integral.

is the one in [9]. Each of the mentioned techniques needs the off-line identification of the inverter parameters. Such identification procedures requires extra processing units, that may be time-consuming and may require non-obvious off-line post-processing.

The commissioning algorithm presented here is very simple and can be implemented with any flux observer or estimator based on back-EMF integration. The method is performed at the drive start-up by injecting a proper set of DC current values along the stator α axis, and it is easily integrated in the starting sequence of the control algorithm.

The proposed identification principle applies to all those sensorless AC drives where the flux is estimated using the back-EMF integration, not only for IM drives but also permanent magnet synchronous motor drives, either of the surface-mounted magnets type (SMPM motor) or the interior permanent magnets motor type (IPM). Moreover, the method can be also integrated into direct-torque control (DTC) algorithms, where the sensitivity to inverter errors at low speed is particularly high [10], [11], but it would require the implementation of vector current regulators for the identification session in this case, since the DTC does not include current vector control.

The goals of the paper are:

- to review the issues of flux estimation at low-speed;
- to review the inverter non-linear model;
- to review the feed-forward compensation of the inverter nonlinearities;
- to propose a method for the inverter model identification, valid for all the flux estimators based on back-EMF integration.

Experimental results are provided to demonstrate the feasibility of the self-commissioning algorithm.

II. Flux Estimation at Low Speed

In many SFOC schemes the estimation of the flux vector, either stator or rotor flux, relies on the time integral of the motor back-EMF [9]. For stator flux oriented control the well known expression (1) is obtained.

$$\hat{\overline{\lambda}}_s = \int \left(\overline{v}_s^* - \tilde{R}_s \overline{i}_s \right) dt \tag{1}$$

Where $\hat{\overline{\lambda}}_s$ is the observed stator flux vector, $\overline{v}_s^*$ is the reference voltage vector, $\overline{i}_s$ is the stator current vector and $\tilde{R}_s$ is the estimated stator resistance.

For rotor flux-oriented control, the rotor flux is obtained from the stator flux as in (2).

$$k_r \cdot \hat{\overline{\lambda}}_r = \int \left(\overline{v}_s^* - \tilde{R}_s \overline{i}_s \right) dt - \sigma L_s \overline{i}_s \tag{2}$$

Where $\hat{\overline{\lambda}}_r$ is the observed rotor flux vector, $k_r = L_m/L_r$ is the coupling factor of the rotor windings, L_m, L_s, L_r are respectively the mutual inductance between stator and rotor windings, the stator inductance and the rotor inductance and $\sigma = 1 - L_m^2/(L_s L_r)$ is the total leakage factor.

A. Flux estimation error

Most of the inaccuracy in (1) and (2) accounts for the voltage and stator resistance estimate terms $\overline{v}_s^*$ and $\tilde{R}_s$. The current measure may also contribute to flux inaccuracy, due to DC offset or gain unbalance between the three phase current measures: all these errors are not considered here since the analog conditioning of the A/D inputs is supposed to be matched and compensated toward temperature drift, while the offset is calculated and compensated at DSP power-up.

Dealing with rotor flux estimation (2), the inductive motor parameters $k_r, \sigma L_s$ give nearly no error: they depend on the actual magnetization current, due to magnetic saturation, but with very low sensitivity. The two terms are accurately modeled as two constants parameters.

Near zero frequency, the motor back-EMF become very low and the effects of voltage and stator resistance estimation errors become more and more relevant for flux orientation. Even with a perfectly matched $\tilde{R}_s$, as far as the stator frequency lowers, the inverter voltage drops introduce a voltage distortion that tend to overcome the fundamental voltage term, leading to the loss of information about the machine flux.

The point here is to compensate for the errors introduced by the inverter non-linear drops in order to obtain an accurate voltage estimation, suitable for robust flux estimation. The stator resistance at start-up is also estimated, similar to off-line estimation proposed in [12]. For maintaining the accuracy when heavy resistance detuning occurs other solutions are capable of updating the resistance estimate during the drive operation [8] and [9].

III. Inverter Model

The inverter modeling has been proposed by several authors [9], [6], [7], [13], with the aim at describing and compensating the voltage error between the command voltage and the actual motor voltage. In particular, a detailed modeling of all the possible sources of voltage distortion can be found in [14]. The main contributions to voltage error are given by:

- inverter dead-time;
- on-state voltage drop of the power switches;
- delay in the actuation of the switch commands (communication line, rise and fall time).
- time delay introduced by the PWM switching period and amplitude error due to PWM resolution.

The last two points have no practical impact on field orientation. The actuation delay is mainly a group delay: the residual error is very small and can be threated by dead-time compensation. Time and numeric discretization are not a problem with up-to-date processors, unless the fundamental frequency is sufficiently lower than the switching frequency.

The inverter error is then dominated by the turn-on dead-time and the on-state voltage drops of the power switches [9], whose effects on flux estimation become evident at low speed.

The actual motor voltage can be expressed as:

$$\overline{v}_s = \overline{v}_s^* + \overline{v}_{dT} + \overline{v}_{on} \tag{3}$$

where $\overline{v}_{dT}$ is the error introduced by the dead-time effects, and $\overline{v}_{on}$ is the on-state voltage drop.

A. Dead-time voltage error ($\overline{v}_{dT}$)

The error introduced by dead-time (4) is a "time-execution" error: the executed duty-cycle of each phase differ from the respective reference value according to the signum of the corresponding phase current. The error depends on the duration of the dead-time respect to the PWM period, and on the dc-link voltage, according to (4):

$$\overline{v}_{dT} = \frac{4}{3} \cdot t_d \cdot f_s \cdot V_{dc} \cdot sign(\bar{i}_s) \tag{4}$$

Where V_{dc} is the dc-link voltage, t_d is the IGBT turn-on dead-time and f_s is the PWM switching frequency. Equation (4) is expressed in the α, β stationary frame. The non linear function $sign(\bar{i}_s)$ has been introduced in [9] and [7] and will be described in the following.

B. On-state voltage error ($\overline{v}_{on}$)

Dealing with the voltage drop of the power switches, the approach is the one proposed in [6]. The model for the IGBT or active switch (sw) and the Free-Wheeling diode (fw) drop is usually made of one constant term (threshold voltage) and one linear term (differential resistance), like in (5) and (6).

$$v_{sw} = V_{th,sw} + R_{sw} \cdot |i_{sw}| \tag{5}$$

$$v_{fw} = V_{th,fw} + R_{fw} \cdot |i_{fw}| \tag{6}$$

For small output voltages of the inverter (duty-cycles ≈ 0.5) the sw and fw drops can be averaged leasing to the model described in (7) and (8), valid for one phase.

$$v_{on} = V_{th} \cdot sign\,(i_x) + R_d \cdot i_x \tag{7}$$

$$\begin{cases} V_{th} = \frac{V_{th,sw}+V_{th,fw}}{2} \\ R_d = \frac{R_{sw}+R_{fw}}{2} \end{cases} \tag{8}$$

Where $x = (a, b, c)$, i_x is the phase current. The vector voltage error in α, β coordinates is:

$$\overline{v}_{on} = \frac{4}{3} \cdot V_{th} \cdot sign(\bar{i}_s) + R_d \cdot \bar{i}_s \tag{9}$$

C. Non linear term

The non linear function $sign(\bar{i}_s)$ introduced in (9), appears also in (4). It has been defined in [7], [9] as the vector signum of the motor phase currents:

$$sign(\bar{i}_s) = \frac{1}{2}\left\{sign(i_a) + e^{j\cdot 2\pi/3} sign(i_b) + e^{j\cdot 4\pi/3} sign(i_c)\right\} \tag{10}$$

where i_a, i_b, i_c are the motor phase currents. The term $sign(\bar{i}_s)$ is a unity-vector ($\left|sign(\bar{i}_s)\right| = 1$) that assumes six positions in the α, β state plane, according to the phase angle of the current vector. It indicates which of the $\pm 30°$ sectors centered around the three phase axes a, b, c is the one where the current vector actually lays. In Fig.2, the non-linear function has been represented in terms of direct and quadrature components respect to the current vector as also done in [7]. The direct component is in phase with the current, and has nearly constant amplitude ($3/\pi$). The average value of the direct component (black thin line in Fig.2) represents the fundamental component of the corresponding voltage drop, in phase with the current. The ripple of the direct part contributes to voltage distortion. The quadrature component has no average value and introduces only distortion at six time the fundamental frequency, that is at the zero-crossing of each phase current. To summarize, the direct component mainly introduces fundamental voltage or amplitude error while the quadrature component introduces the most part of the distortion.

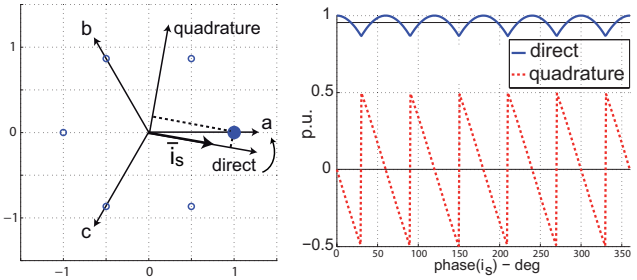

(a) (b)

Fig. 2. Representation of the vector signum function $sign(\bar{i}_s)$. a) The six dots are the instantaneous values of $sign(\bar{i}_s)$ in the stationary frame. b) The direct and quadrature components of $sign(\bar{i}_s)$ are represented with respect to the position of the motor current vector $\bar{i}_s$. Direct and quadrature components are defined in subfigure (a) for a given current vector position. Phase zero coincides with the current vector aligned to phase a.

D. Overall inverter error

Despite dead-time $\overline{v}_{dT}$ and on-state voltage drops $\overline{v}_{on}$ have completely different natures, the former being a time-error and the latter a voltage drop in series with the motor, their effects on the inverter voltage are similar and mainly non-linear. According to (4) and (7), the two error terms can be grouped together, thus equation (3) can be expressed as (11).

$$\overline{v}_s = \overline{v}_s^* + R_d \cdot \bar{i}_s + \frac{4}{3} \cdot V_{th}^{'} \cdot sign(\bar{i}_s) \tag{11}$$

Where:

$$V_{th}^{'} = V_{th} + t_d \cdot f_s \cdot V_{dc} \tag{12}$$

The equivalent threshold $V_{th}^{'}$ includes the effect of both dead-time and on-state threshold voltage. The differential resistance R_d is in series with the motor resistance: in the following R_s and R_d will be incorporated into the unique parameter $\tilde{R}_s$ that accounts for the overall series resistance of the drive. If the size of the inverter and the motor are properly matched, R_d is small with respect to R_s.

E. Effects of the error with scalar control

When sinusoidal reference voltages are imposed, like for example in V/Hz scalar control, the actual motor voltage is deformed according to (11) and produces current deformation,

torque ripple and even control instability [15]. The distortion of the actual voltage trajectory in the α, β plane with respect to the reference voltage circle is simulated in Fig.3 for different load situations and disregarding the resistive R_d term in (11). It can be noticed that at given reference voltage amplitude (1 p.u.) and inverter error $V_{th}^{'}$ (0.25 p.u.), the motor voltage trajectory depends on the power factor. In particular, zero power factor (dashed line) and 0.7 power factor (continuous line) are illustrated in the plots, and are representative of no-load and load operation respectively. At no-load the non linear error distorts the voltage path but gives no amplitude error, as can be seen from the dashed trajectories that move around the circle both in Fig.3-a and -b. This means that the motor voltages will be affected only by a distortion at six times the fundamental. As long as the power factor increases, the voltage drop due to the direct component introduced in Fig. 2 arises, as shown by the decreasing (or increasing) amplitude of the voltage trajectory in Fig.3-a (or -b): apart for the distortion, in motoring operation the voltage path tends to become smaller as the load increases, and the opposite happens in generator operation, like for a series-type voltage drop. Nevertheless, the most visible effect in case of scalar control is the heavy current deformation at low speed, whose typical waveform is reported in Fig. 4.

F. Effects of the error with current vector control

In current controlled drives, like Field Oriented Controlled drives, the fast response of the current regulators deforms the reference voltage in order to keep the currents sinusoidal. In this case the motor voltages are sinusoidal and the reference voltages are deformed instead. If such deformed signals are used for flux estimation, both the amplitude error and the harmonic distortion that affect the voltages are reflected onto the flux estimate. At low speed the voltage reference distortion becomes evident in comparison with the fundamental motor voltage, and gives a relevant flux estimation error. The estimated flux is also deformed, and field orientation becomes inaccurate. In order to improve the flux estimation and obtain robust flux orientation as far as possible at low speed, the inverter error must be compensated, as described in the following section. The reference voltages with and without compensation for the IM drive under test are given in Fig. 9, in the Experimental Results section.

IV. Feed-forward compensation and self-commissioning algorithm

The non linear part of the inverter error (11), that accounts for both dead-time and on-state threshold drops, is compensated in feed-forward as depicted in Fig.5. If the compensation is correct, the current regulators do not need to compensate for such error, and the voltage signals $before$ the feed-forward add point ($\overline{v}_s^*$ in Fig.5) are sinusoidal and suitable for flux estimation. The accuracy of the voltage compensation is demonstrated by the circular path of the reference voltage signals in steady state, as in Fig.9.

The compensation method adopted here is the same proposed in [8], except for the calculation of the $sign(\overline{i}_s)$ function that is here implemented in the three- phase reference frame and not in the two-phase stationary frame. The signum of the three phase currents are evaluated and the phase reference voltages are corrected accordingly, as also proposed in [13]. Apart for implementation details, the results of the compensation are the same documented in [6] and [7], where hardware feed-forward compensation is provided by means of a proper lead time of IGBT commands.

The equivalent voltage threshold $V_{th}^{'}$ defined in (12) and the overall series resistance estimate $\tilde{R}_s$ $(= R_s + R_d)$, where R_d has been introduced in (11), can be estimated by means of the feedback signal $\overline{v}_\epsilon$ of the flux observer defined in Fig.1. The

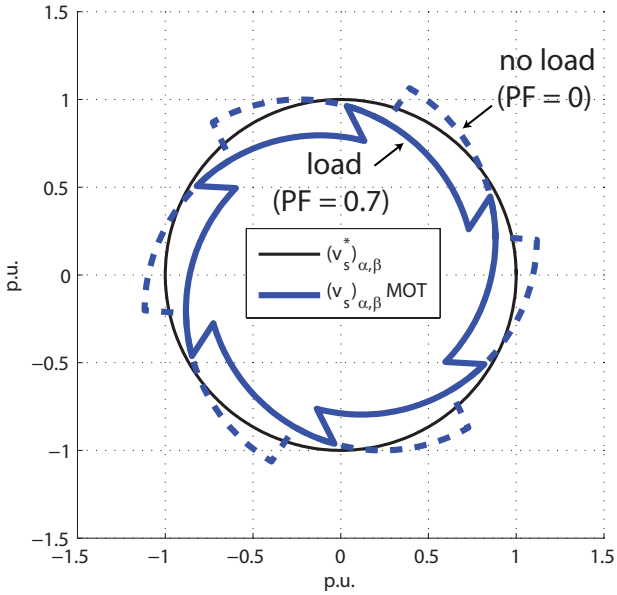

(a) MOTOR OPERATION

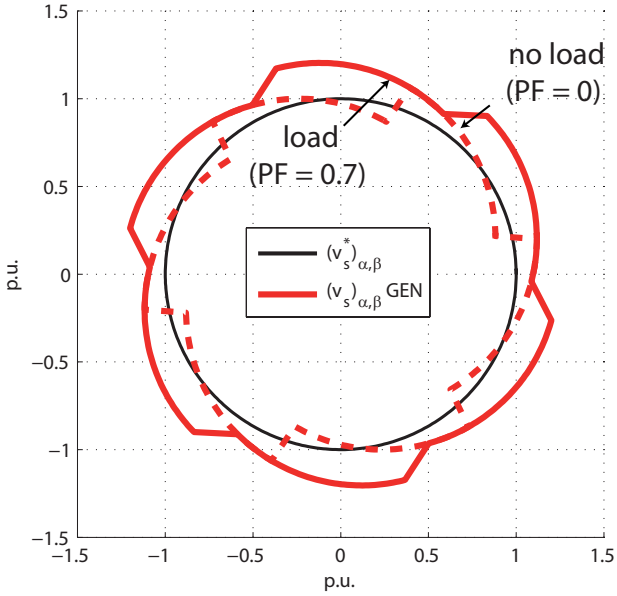

(b) GENERATOR OPERATION

Fig. 3. Voltage distortion in scalar control at different Power Factors, per-unit simulation. Represented PF values are 0 (dashed), corresponding to no-load operation and 0.7 (continuous), corresponding to load operation.

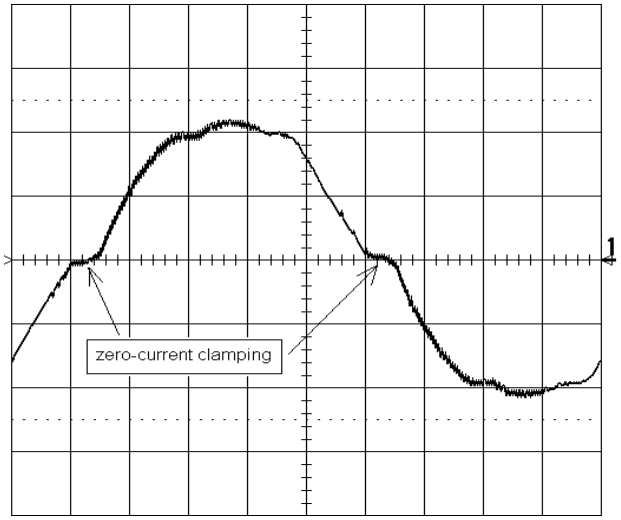

Fig. 4. Effects of inverter nonlinearity at impressed sinusoidal voltage. Voltage control, $|v_s|$ = 10 V, 5.0 Hz. Timebase: 20 ms/div. Scale factor: 1.0 A/div

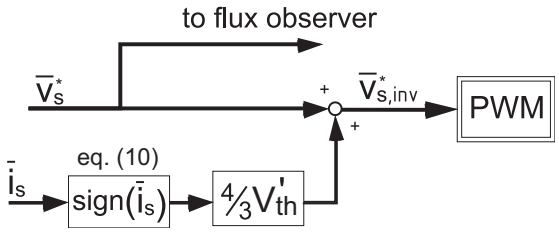

Fig. 5. Feed-forward compensation of the inverter nonlinearity.

identification can be performed at the drive start-up and does not require the knowledge of the implemented dead-time or any data-sheet information about the adopted power switches. The flux observer adopted for the experiments is the Voltage-Current Rotor flux observer (VIRO) for low cost applications presented in [16] and reported in Fig. 6, but the method is valid for all the observers based on back-EMF integration, either rotor or stator field oriented, according to the general form estimator reported in Fig.1.

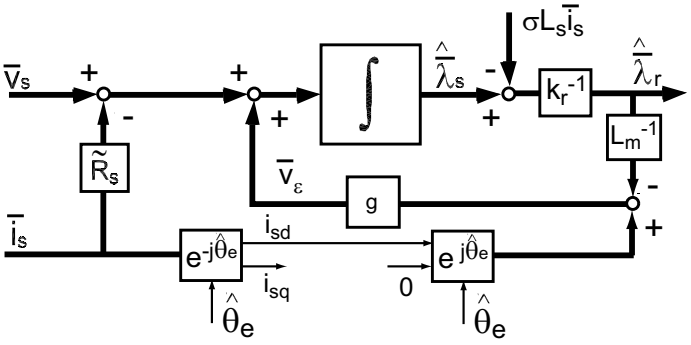

Fig. 6. Block scheme of the closed-loop VI rotor flux observer (VIRO) adopted in the experiments [16]. θ_e is the position of the observed rotor flux.

In DC steady state conditions the back-EMF is zero and thus the motor voltage equals the resistive drop (13).

$$\overline{v}_s = R_s \cdot \overline{i}_s \tag{13}$$

With no dead-time compensation, once the flux estimator transient is extinguished, the input of the back-EMF integrator of Fig. 1 converges to zero (14).

$$\overline{v}_s^* - \tilde{R}_s \cdot \overline{i}_s + \overline{v}_\epsilon = 0 \tag{14}$$

By substituting (11) and (13) into (14), the feedback signal puts in evidence the two error terms evidenced in (15).

$$-\overline{v}_\epsilon = \frac{4}{3} V_{th}^{'} \cdot sign(\overline{i}_s) + (R_d + \Delta R_s)\overline{i}_s \tag{15}$$

Where ΔR_s is the estimation error of the stator resistance ($R_s = \tilde{R}_s + \Delta R_s$). In steady state DC conditions, the feedback signal equals the inverter error plus the motor resistance estimation error. In the following, the two terms (linear and non linear) of (15) will be separated and separately compensated.

A. Step 1: evaluation of $V_{th}^{'}$

For very little values of DC current, the resistive term in (15) is negligible, since both the current amplitude and the differential resistance term $\Delta R_s + R_d$ are small. In particular, a current vector such as $\overline{i}_1 = I_1 + j0$ (aligned with the α axis), of proper amplitude I_1, puts in evidence the inverter non-linear term:

$$-\overline{v}_\epsilon \cong \frac{4}{3} V_{th}^{'} (1 + j \cdot 0) \qquad \overline{i}_s = (I_1 + j \cdot 0) \tag{16}$$

A low current value can be used for setting the gain $V_{th}^{'}$ of the dead-time compensation.

B. Step 2: Evaluation of $R_d + R_s$

With the $V_{th}^{'}$ compensation active and tuned according to step 1, the $sign()$ term disappears from (15). Now a larger value of DC current can be supplied to the motor in order to put in evidence the the overall series resistance:

$$-\overline{v}_\epsilon \cong (R_d + \Delta R_s)(I_2 + j \cdot 0) \qquad \overline{i}_s = (I_2 + j \cdot 0) \tag{17}$$

In this case, the resistance estimation error can be estimated and compensated.

C. Closed-loop identification procedure.

The block-scheme of the self-commissioning algorithm is reported in Fig.7, while the waveforms of the identification procedure are reported in Fig.8. The motor and the inverter data are reported in the Appendix.

At the start-up of the drive, the gain of the feed-forward compensator $V_{th}^{'}$ is initialized to zero (no compensation), while the stator resistance estimate is set to its nameplate value. The flux position is initialized to zero and then the d, q axes coincide with the stator α, β axes.

At first (step 1), the small DC current $\overline{i}_1 = 0.3A + j0$ is set by the current control for $800ms$. The integrative regulator with gain k in Fig.7 corrects the value of $\tilde{V}_{th}^{'}$ in order to

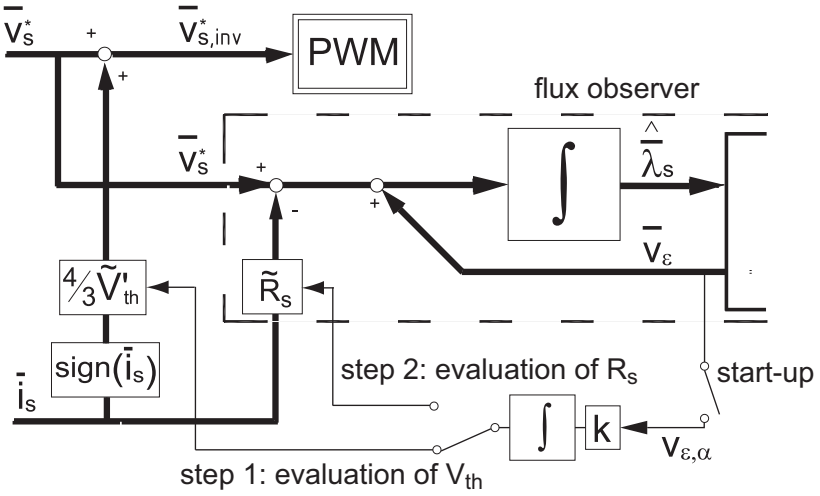

Fig. 7. Algorithm for the self-commissioning of the inverter non-linearity compensation. $V_{th}^{'}$ is feed-forward compensated, R_d incorporated in the flux-observer parameter $\tilde{R}_s$.

cancel $v_{\epsilon\alpha}$. When $v_{\epsilon\alpha}$ convergers to zero it means that the compensation is correct ($\tilde{V}_{th}^{'} \cong V_{th}^{'}$), according to (16).

With the dead-time compensation activated according to the results of step 1, a second current value $\bar{i}_2 = 3.5A + j0$ of larger amplitude is set (step 2). As I_1 is very small for having practical zero resistive drop, the pulse I_2 should be as large as possible, according the inverter current rating. Again, the integrative regulator corrects the parameter $\tilde{R}_s$ in the flux-observer until the feedback signal $v_{\epsilon\alpha}$ convergers to zero. At the end of the second current step, the flux observer is capable of estimating the flux with no error and the drive is ready to start.

The identification procedure takes $1.6s$ overall in the reported example (Fig.8). The time required by the procedure to converge with different drives depends on the gain of the back-EMF integrator in the flux-observer: the lower is the gain, the slower is the convergence.

The cost of the implementation in terms of design and code lines is extremely limited. The only parameter to be tuned is the gain k of the regulator: if the gain is too large the evolution becomes oscillatory. The algorithm is suitable for fixed-point implementation as demonstrated in the following section.

V. Experimental Results

The self-commissioning algorithm has been experimentally tested with the IM drive described in the Appendix. The experimental tests have been carried out with a 16-bit fixed-point DSP, suitable for industrial drives. As mentioned before, the adopted flux observer (Fig.6) is the the one indicated as VIRO presented in [16].

The identification procedure is shown in Fig.8, for two different temperatures of the stator windings, 20°C and 80°C respectively. It must be noted that the obtained $\tilde{V}_{th}^{'}$ value is not affected by the stator temperature, while the term $\tilde{R}_s$ converges to different values, according to the stator temperature.

In Fig.9 the effect of feed-forward compensation is evidenced at very low speed, no load (25 rpm that corresponds to 0.42 Hz electrical frequency). The no-load test refers to current-control at a given reference frequency, and not to SFOC, in order to put in evidence the effect of compensation without modifying the operation of the drive. If the compensation is not enabled, the reference voltages exhibit distorted waveforms (Fig.9-a) as also evidenced by the estimated electrical speed that is obtained from the external product of the estimated stator flux and the estimated back-emf according to the method proposed in [16]. When the feed-forward compensation is enabled, the electrical speed distortion is strongly reduced and the voltage commands become nearly sinusoidal apart for a little residual disturbance at 6-time the fundamental frequency (Fig.9-b).

In Fig.10 the rotor flux estimation is presented in speed-controlled SFOC at 100 rpm. Uncompensated (a) and compensated (b) situations are reported. The baseline for comparison are the flux components obtained by a sensored observer of the VIθ_r type [17] that is run in background by the controller, while the sensorless observer is used for field orientation. The voltage signals used by the sensored observers are not compensated toward inverter errors in both figures. The flux components are represented in stator coordinates. The positive effects of feed-forward compensation can be summarized in three points:

- the rotor flux distortion (single components and amplitude) is strongly reduced and comparable with that of the sensored observer;
- the rotor flux amplitude is correctly estimated when the compensation is ON, while overestimated with no compensation;
- with the compensation ON, the flux position is practically not distorted and nearly coincides with the sensored one. Moreover, the better field orientation of subfigure (a) respect to subfigure (b) is also demonstrated by the lower electrical frequency of the latter with respect to the former, that means that with the compensation the IM runs at a lower slip frequency for a given mechanical

speed, so it is better oriented.

The stator resistance estimation obtained with this procedure is correct at the start-up only. In case the continuous, real-time estimation of the stator resistance is necessary, some effective methods can be found in the literature [8], [9].

In Fig.11 the complete start-up sequence of the drive is reported: the self-commissioning of the inverter and stator resistance model is performed within a couple of seconds ($1.6s$ in the example) and then a speed ramp is commanded in speed-controlled SFOC. The motor speed ramp is smooth and regular. The actual speed is represented in the figure, measured by means of an incremental encoder.

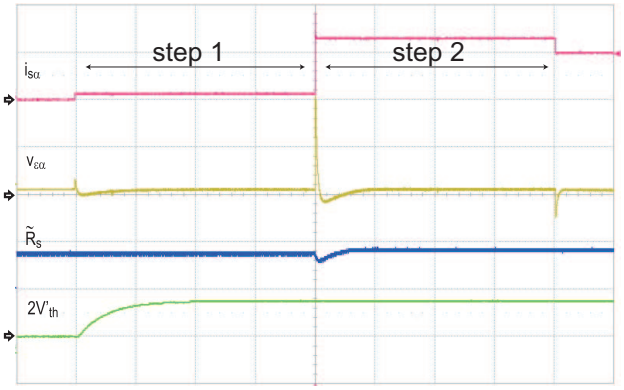

(a) Cold windings (20°C), 200ms/div

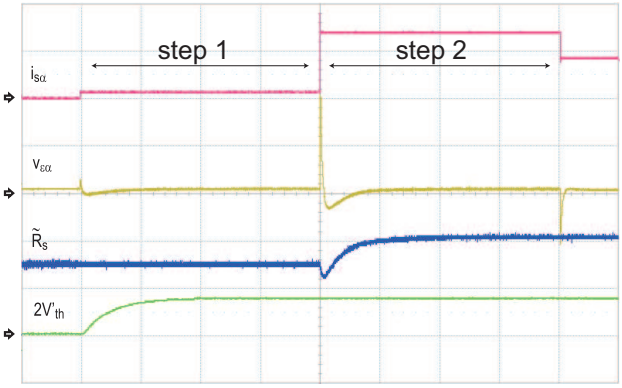

(b) Hot windings (80°C), 200ms/div

Fig. 8. Identification procedure at different winding temperatures, I_1 = 0.3 A, I_2 = 3.5 A. Scale factors, from top to bottom: 2.5 A/div, 52.5 V/div, 2.1 Ω/div, 10.5 V/div.

VI. Conclusions

The paper proposes a simple solution for the identification and compensation of the inverter error in Sensorless Field Oriented Controlled IM drives. The parameters of the inverter model are evaluated at the drive start-up by means of the flux observer/estimator feedback signal. No information about dead-time duration or power switch data-sheet is needed. No off-line calculation is required and the overall procedure stays within a couple of seconds for any drive size. The initial value of the motor stator resistance is also estimated. The method applies to any flux estimator/observer based on back-emf integration, and it is valid also for other types of AC drives (e.g. permanent magnet synchronous motor drives). The experimental results demonstrate the feasibility of the proposed method for a SFOC IM drive.

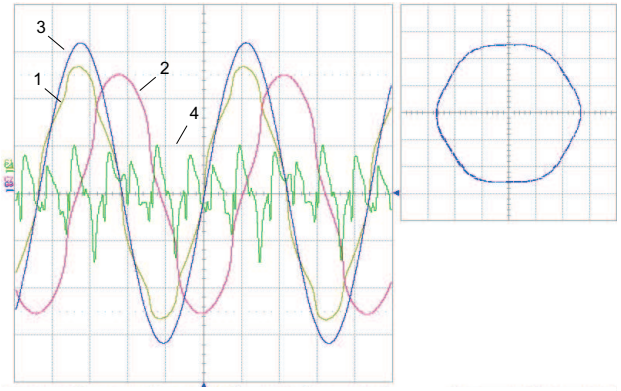

(a) Compensation OFF, 500ms/div

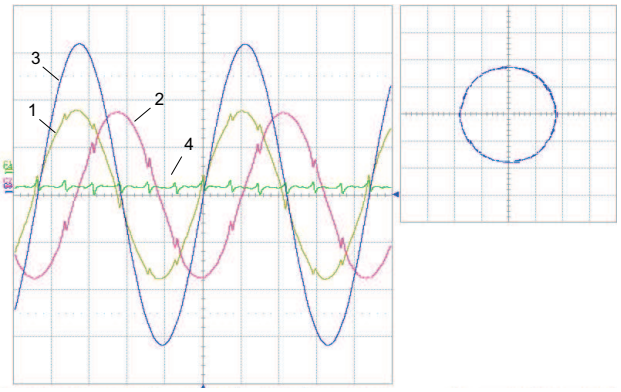

(b) Compensation ON, 500ms/div

Fig. 9. No-load test, 25 rpm. Effect of the inverter error on the reference voltage signals and on the estimated electrical speed for different compensation situations. Scale factors: 1: $v_{s,\alpha}$ (4.5 V/div), 2: $v_{s,\beta}$ (4.5 V/div), 3: $i_{s,a}$ (0.7 A/div), 4: ω_e (180 rpm/div)

Appendix

The motor under test is rated as follows: 820 W, 195 V/60 Hz, 5 A, 2 poles, 17000rpm max speed. Stator Resistance: 3.64 Ω at 75°C. The inverter rating is: 220V, 50Hz single-phase input, passive rectifier. Intelligent-Power-Module SOA: 600V, 10A. Dead-time duration is 1μs. The DSP is a Freescale 56F8323. The observer gain is set for having a cross-over frequency of 35rad/s between the rotor model and the stator model [16]. The base quantities used for machine model normalization for the fixed-point DSP implementation are: base voltage Vbase=525 V, base current Ibase=12.5 A, base electrical speed ωbase=2·π·500 (rad/s) and the base flux λbase=0.67 Vs computed as λ base = 4· Vbase / ωbase.

References

[1] K.Hurst, T.Habetler, G.Griva, and F.Profumo. Adaptive speed identification for vector control of induction motors without rotational transducers. *IEEE Transactions on Industry Applications*, 28(5):1054 – 1061, 1992.

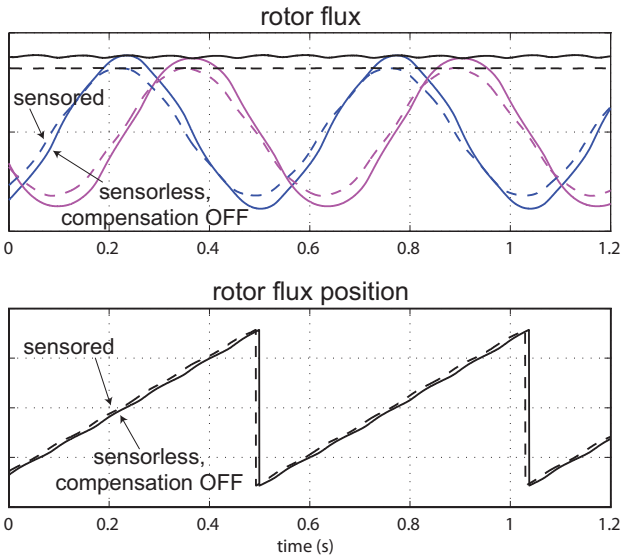

(a) Compensation OFF

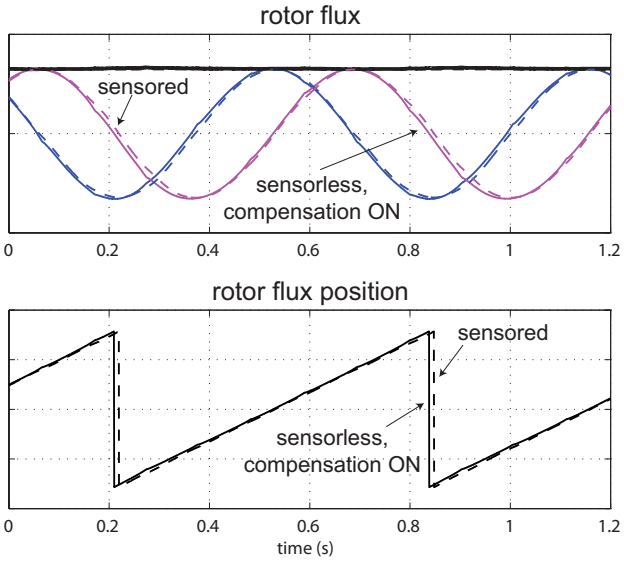

(b) Compensation ON

Fig. 10. No-load test, 100 rpm. Effect of the inverter error on the observed rotor flux (top subplot) and flux orientation (bottom subplot) for different compensation situations. The rotor flux components in the α, β stationary frame are represented, together with the observed flux amplitude. The sensorless observer is compared with a sensored $VI\theta_r$ observer [17], for the sake of evidencing the inverter error effects. Scale factors: 0.5 Vs/div, 2 rad/div.

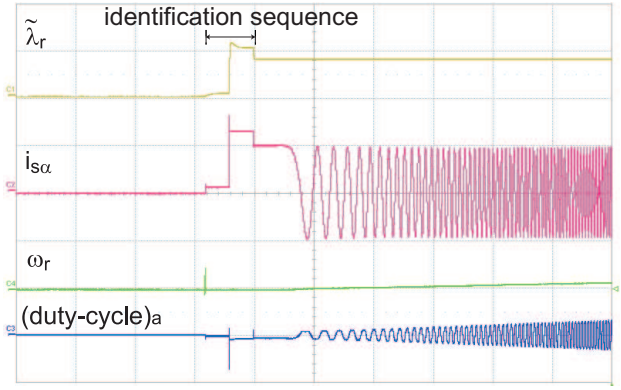

Fig. 11. Start-up of the drive: self-commissioning of $V_{th}^{'}$ and R_d and speed ramp. Timebase: $1s/div$, Scale factors, from top to bottom: 0.33 Vs/div, 2.5 A/div, 15000 rpm/div, 1/div.

[2] C.Schauder. Adaptive speed identification for vector control of induction motors without rotational transducers. *IEEE Transactions on Industry Applications*, 28(5):1054 – 1061, 1992.

[3] H.Kubota, K.Matsuse, and T.Nakano. Dsp-based speed adaptive flux observer of induction motor. *IEEE Transactions on Industry Applications*, 29(2):344 – 348, 1993.

[4] S.Doki, S.Sangwongwanich, T.Yoenmoto, and S.Okuma. Speed-sensorless field-oriented control using adaptive sliding mode observers. In *IECON Conference Records*, pages 453 – 458, 1990.

[5] C. Lascu and Gh.-D. Andreeescu. Sliding-mode observer and improved integrator with dc-offset compensation for flux estimation in sensorless-controlled induction motors. *IEEE Transactions on Industrial Electronics*, 53(3):785 – 794, 2006.

[6] J.Choi and S.Sul. Inverter output voltage synthesis using novel dead time compensation. *IEEE Transactions on Power Electronics*, 11(2):221 – 227, 1996.

[7] S.Bolognani and M.Zigliotto. Self-commissioning compensation of inverter non-idealities for sensorless ac drives applications. In *Proc. of Power Electronics, Machines and Drives*, volume IEE, pages 30–36, 2002.

[8] J.Holtz and J.Quan. Drift- and parameter-compensated flux estimator for persistent zero-stator-frequency operation of sensorless-controlled induction motors. *IEEE Transactions on Industry Applications*, 39(4):1052 – 1060, 2003.

[9] J.Holtz and J.Quan. Sensorless vector control of induction motors at very low speed using a nonlinear inverter model and parameter identification. *IEEE Transactions on Industry Applications*, 38(4):1087 – 1095, 2002.

[10] Li Yongdong, Shao Jianwen, and Si Baojun. Direct torque control of induction motor for low speed drives considering discrete effects of control and dead-time of inverter. In *Industry Applications Conference, 1997. Thirty-Second IAS Annual Meeting, IAS '97., Conference Record of the 1997 IEEE*, volume 1, pages 781–788 vol.1, Oct 1997.

[11] D. Casadei, G. Serra, A. Tani, L. Zarri, and F. Profumo. Performance analysis of a speed-sensorless induction motor drive based on a constant-switching-frequency dtc scheme. *Industry Applications, IEEE Transactions on*, 39(2):476–484, Mar/Apr 2003.

[12] H. Schierling. Fast and reliable commissioning of ac variable speed drives by self-commissioning. In *Proc. of IEEE Industry Applications Society Annual Meeting*, pages 489 – 482, 1988.

[13] J.K.Pedersen, F.Blaabjerg, J.W.Jensen, and P.Thogersen. An ideal pwm-vsi inverter with feedforward and feedback compensation. In *Conf. Rec. EPE*, pages 501–507, 1993.

[14] R.J. Kerkman, D. Leggate, D.W. Schlegel, and C. Winterhalter. Effects of parasitics on the control of voltage source inverters. *Power Electronics, IEEE Transactions on*, 18(1):140–150, Jan 2003.

[15] D. Leggate and R.J. Kerkman. Pulse-based dead-time compensator for pwm voltage inverters. *Industrial Electronics, IEEE Transactions on*, 44(2):191–197, Apr 1997.

[16] G.Pellegrino, R.Bojoi, and P.Guglielmi. Performance comparison of sensorless field oriented control techniques for low cost three-phase induction motor drives. In *Proc. of IEEE Industry Applications Society Annual Meeting*, pages 281 – 288, 2007.

[17] P.L. Jansen and R.D. Lorenz. A physically insightful approach to the design and accuracy assessment of flux observers for field oriented induction machine drives. *Industry Applications, IEEE Transactions on*, 30(1):101–110, Jan/Feb 1994.

[18] J.Holtz. Sensorless control of induction motor drives. *Proceedings of the IEEE*, 90(8):1359 – 1394, 2002.

[19] R.Bojoi, P.Guglielmi, and G.Pellegrino. Sensorless direct field oriented control of three-phase induction motor drives for low cost applications. In *Proc. of IEEE Industry Applications Society Annual Meeting*, pages 866 – 872, 2006.

Gianmario Pellegrino (M06) received the M.Sc. and Ph.D. degrees in electrical engineering from the Politecnico di Torino, Turin, Italy, in 1998 and 2002, respectively. Since 2002 he is with the Department of Electrical Engineering, Politecnico di Torino, first as Research Associate and as Assistant Professor from 2007. He has been teaching power electronics and electric drives. He is involved in research projects for the public sector and for private groups, he has more than 30 technical papers and one international patent. His areas of interest are the electric drives, namely, in the motor design and digital control. He works in the fields of electric traction and of the design of direct-drive generators for wind energy production. He has been a Guest Researcher at Aalborg University, Denmark, in 2002.

Eric Armando was born in Cuneo, Italy, in 1974. He received the M.Sc. and Ph.D. degrees in electrical engineering from the Politecnico di Torino, Turin, Italy, in 2002 and 2008, respectively. He is now with Politecnico di Torino as a Research Assistant. He has been in charge of national research projects, funded by the Italian Research Ministry board, in the field of ac drives. His fields of interest are power electronics and high-performance AC motor drives.

Paolo Guglielmi (M07) was born in Imperia, Italy, in 1970. He received the M.Sc. degree in electronic engineering and the Ph.D. degree in electrical engineering from the Politecnico di Torino, Turin, Italy, in 1996 and 2001, respectively. In 1997, he joined the Department of Electrical Engineering, Politecnico di Torino, where he became a Researcher in 2002. He has authored several papers published in technical journals and conference proceedings. His fields of interest include power electronics, high-performance servodrives, and computer-aided design of electrical machines. Dr. Guglielmi is a Registered Professional Engineer in Italy.

Radu Iustin Bojoi (M06) received the M.Sc. degree in Electrical Engineering from the Technical University "Gh. Asachi" Iasi, Romania, in 1993, and the Ph.D. degree from Politecnico di Torino, Italy, in 2003. Since 1994-1999 he was an Assistant Professor in the Department of Electrical Drives and Industrial Automation from Technical University of Iasi. In 2004 he joined the Department of Electrical Engineering of the Politecnico di Torino as an Assistant Professor. His scientific interests regard the design and development of DSP- and FPGA-based advanced control systems in the fields of power electronics, high-performance electrical drives and power-conditioning systems. He has published more than 60 papers in international conferences and technical journals. Dr Bojoi has received the IPEC First Prize paper Award in 2005.